CHAPTER 104

STABILITY OF ARMOR STONES OF A SUBMERGED WIDE-CROWN BREAKWATER

Norimi MIZUTANI,[1] Teofilo Monge RUFIN Jr.,[2] and Koichiro IWATA [3]

Abstract

The stable weight of armor rubbles of a submerged wide-crown break-water was analyzed in relation to the wave force acting. At first, stability models for armor rubble were derived based on the idealized spherical armor unit; then, the shape effect of armor stones on acting wave forces and stability was investigated experimentally. Based on the results, the proper modification of the stability models for spherical armor unit gives good estimate of the stable weight of armor rubbles. Furthermore, the shape effect on wave forces and stability is significant; whereas, the shape effect of armor rubble on the stable weight is relatively small.

1. INTRODUCTION

The submerged breakwater is a nature-conscious coastal protection work which takes the essential role in providing an agreeable environment of safety in coastal areas. This structure creates a calm sea and scarcely harms the coastal scenery nor obstruct the utilization of the sea for recreational and residential developments. In the design of submerged breakwater, an accurate estimation of stable weight of armor unit is deemed necessary. The stable weight of a rubble structure such as the rubble-mound breakwaters (e.g., Hudson et al. 1958, 1959; Hedar 1986), composite rubble-mound breakwater (Brebner and Donnelly 1962), and artificial reef (Uda et al. 1989) were discussed and stability models were subsequently proposed. Most of the existing stability formulae are intended to correlate the stable weight with the wave height, and the relation between the stable weight and wave forces acting have not been discussed in detail. However, the stable weight of the armor unit depends largely on the acting wave forces; thus, it is necessary to relate the stability to the acting wave forces and its pertinent characteristics. Although there have been some studies

[1] Assoc. Professor, D. Eng., Dept. of Civil Eng., Nagoya Univ., Nagoya 464-01, JAPAN
[2] Graduate Student, M. Eng., Dept. of Civil Eng., Nagoya Univ., Nagoya, JAPAN
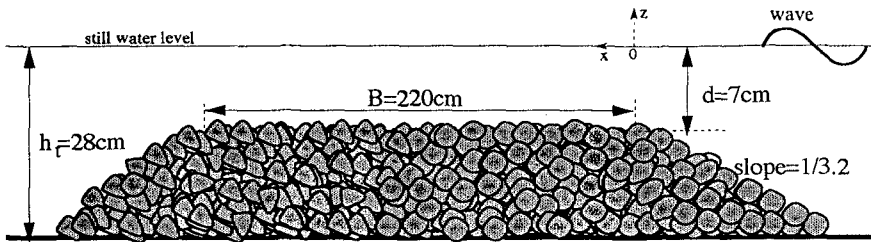[3] M. ASCE, Professor, D. Eng., Dept. of Civil Eng., Nagoya Univ., Nagoya, JAPAN

Figure 1: Schematic diagram of submerged wide-crown breakwater.

Table 1 Characteristics of sample armor stones.

CLASS	SHAPE	D (cm)	D /d	W (g)	S_1/S_2	L_1/L_2
A	sphere	2.47	0.353	19.6	1.0	1.0
	round-type				1.67	1.21
	flat-type				3.01	1.77
	edged-type				2.85	1.22
B	sphere	1.94	0.277	9.5	1.0	1.0
	round-type				1.62	1.48
	flat-type				3.14	1.43
	edged-type				1.87	0.98
C	sphere	1.65	0.236	6.2	1.0	1.0
	round-type				1.62	1.31
	flat-type				2.84	2.38
	edged-type				1.56	0.94

on wave forces acting on rubble stones of a rubble-mound slope breakwaters
(Iwata et al. 1985; Tørum 1994), still the accumulated knowledge on wave
force on rubble stones are very limited because of the complexity of the shape
of stones. The present authors analyzed the wave force acting on a spherical
armor unit which is an ideal shape of rubble stone, and then discussed and
proposed a model for the stable weight in relation to the acting wave force
(Mizutani et al. 1992; Rufin et al. 1993). This method, however, cannot be
directly applied for the case of actual rubble stones without first clarifying the
shape effect of rubble stone on stability and wave force. Hence, this paper
aims to present the wave force and stability of armor stones in relation to the
shape effect, and then develop a method of evaluating the stable weight of
armor rubble of a submerged wide-crown breakwater.

2. EXPERIMENTAL SET-UP AND PROCEDURE

    The stability tests and the laboratory observations of wave forces acting
on spherical armor unit and armor rubble stones on a submerged breakwater
were carried out using an indoor wave tank (25m long x 0.7m wide x 0.9
m deep). The model of the breakwater was prepared using spheres and then
performed with one made of natural stones, as shown in Fig. 1. Regular waves
with different wave periods ($T = 1.0$, 1.4, and 1.8s) were generated in this
experiment.

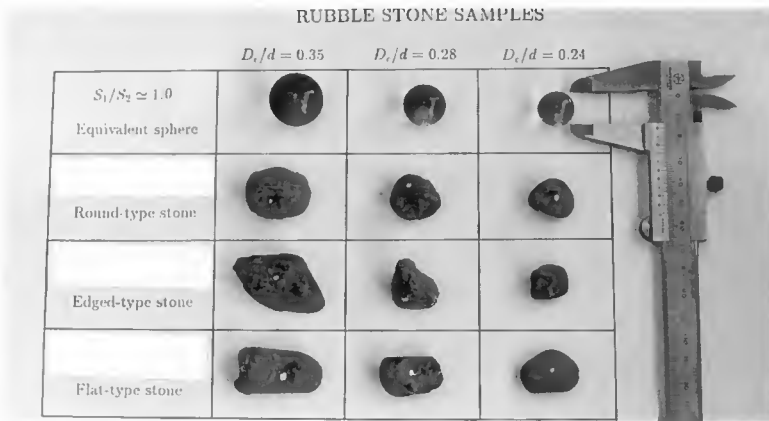   For the stability measurement, the critical wave height of each sample of

Figure 2: Stones samples.

armor unit in each wave period was determined for every designated locations on the submerged breakwater. The critical wave height is defined as the minimum wave height required to move a given sample of armor unit. The samples of armor units were spheres with $D/d = 0.35$, 0.28, and 0.28 and stones, as shown in Fig. 2, with the same volume with that of the equivalent sphere of three different shapes (round-type, flat-type, and edged-type), where D is the diameter of sphere and d is the crown water depth. Table 1 gives the characteristics of the sample armor units used in the investigation, where S_1 and S_2 are the maximum and minimum lengths, respectively, and L_1 and L_2 are the maximum tangential and normal lengths, respectively. The determination was made by generating series of experimental trials with different values of wave height until the critical wave height is attained. The armor sample was placed on the structure surface with the maximum cross-section parallel to the horizontal plane and the minimum cross-section normal to the wave incident direction.

For wave force measurement, the horizontal and vertical wave forces (Fx, Fz) of each sample were measured for a given incident wave height (H_I) and critical wave height conditions. The corresponding water surface elevations and horizontal and vertical water particle velocities (u and w) were also measured. Table 2 gives the experimental conditions. The wave forces were measured for the same placement except for a very small gap between the wave force meter and the surface of the structure. In the measurement of wave force acting on rubble stones, a prototype of the actual stone of interest with exactly the same shape was prepared by plaster cast and used as sensor on the wave force meter.

3. WAVE FORCE ACTING ON ARMOR UNIT

Regardless of wave period, shape, and size of armor units, the nondimen-

Table 2 Experimental conditions.

	h_t/L	0.203	0.131	0.098
x/L	sloping side	-0.304 -0.150 -0.101 0.0	-0.203 -0.152 -0.102 -0.051 0.0	-0.152 -0.103 -0.051 0.0
	crown side	0.101 0.203 0.304 0.506 0.761 1.017 1.268 1.523	0.051 0.102 0.152 0.203 0.307 0.508 0.765 1.021	0.051 0.103 0.204 0.308 0.512 0.767

mensional maximum wave force, $Fx_m/\rho g D^2 H_I$, shows similar variation with the dimensionless distance, x/L, where ρ is the density of water, g is the gravitational acceleration, x is the horizontal distance referred form the leading crown-edge, positive in onshore direction, and L is the wavelength at the toe of the structure. As shown in Fig. 3, $Fx_m/\rho g D^2 H_I$ increases with x/L and H_I/h_t on the slope ($x/L < 0$) and attains a maximum value near the crown-edge (Rufin et al. 1994), where h_t is the still water depth at the toe of the structure. On the crown ($x/L > 0$), $Fx_m/\rho g D^2 H_I$ decreases rapidly for wave breaking condition; whereas, $Fx_m/\rho g D^2 H_I$ decreases gradually for non-breaking condition. Therefore, the nondimensional maximum wave force, $Fx_m/\rho g D^2 H_I$, for non-breaking condition is larger than the wave breaking condition. This may be attributed to the disturbance due to the wave breaking and higher harmonic wave component generated on the crown. Similar tendency was observed for nondimensional maximum wave force in the vertical direction, $Fz_m/\rho g D^2 H_I$, however, the variation with x/L and H_I/h_t is not clear as compared with the horizontal wave force. Moreover, the figure shows that the onshore wave force is generally larger than the offshore wave force.

The shape effect of stones is not sensitive in the variations of nondimensional wave forces with x/L. However, shape effect is very significant on the magnitude of wave forces. Figure 4 gives the comparison of wave force among various shapes of armor unit. For the horizontal wave force, the wave force on round-type stone is almost the same magnitude with the equivalent sphere. The wave force on edged-type stone, however, is much larger than the sphere and round-type stone. For edged-type shape, flow separation takes place easier than the round-shape body because of the edges of stone, consequently, resulting to a larger drag force. On the other hand, the horizontal wave force on flat-type stone is generally small compared to the other types of stones. The method of placement wherein the smallest cross-sectional area faces the horizontal flow gives the flat-type stone the smallest projected area which results to a smaller horizontal wave force. However, the vertical wave force on flat-type stone is much larger than the other types of stone, because of very large projected area. This significant property is attributed to the variation of
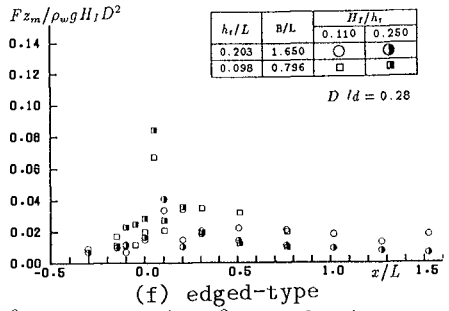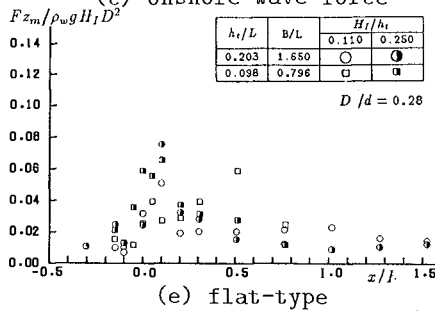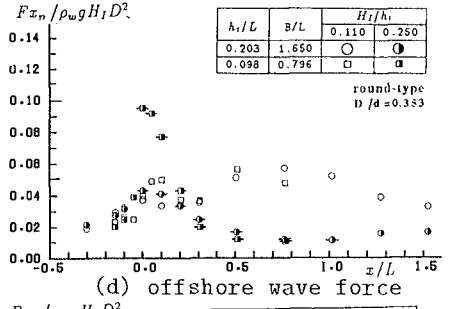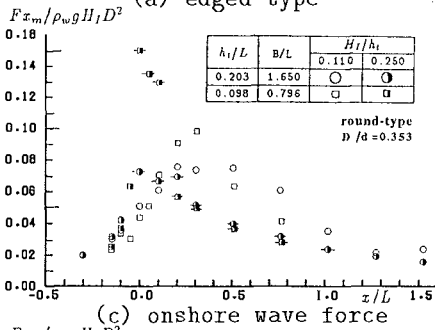
$Fx_m/\rho_w g H_I D^2$

h_t/L	B/L	H_I/h_t	
		0.110	0.250
0.203	1.650	○	◑
0.098	0.796	□	◪

$D/d = 0.28$

------- :non-breaking wave condition
——— :breaking wave condition

(a) edged-type

$Fx_m/\rho_w g H_I D^2$

h_t/L	B/L	H_I/h_t	
		0.110	0.250
0.203	1.650	○	◑
0.098	0.796	□	◪

$D/d = 0.28$

------- :non-breaking wave condition
——— :breaking wave condition

(b) flat-type

$Fx_m/\rho_w g H_I D^2$

h_t/L	B/L	H_I/h_t	
		0.110	0.250
0.203	1.650	○	◑
0.098	0.796	□	◪

round-type
$D/d = 0.353$

(c) onshore wave force

$Fx_n/\rho_w g H_I D^2$

h_t/L	B/L	H_I/h_t	
		0.110	0.250
0.203	1.650	○	◑
0.098	0.796	□	◪

round-type
$D/d = 0.353$

(d) offshore wave force

$Fz_m/\rho_w g H_I D^2$

h_t/L	B/L	H_I/h_t	
		0.110	0.250
0.203	1.650	○	◑
0.098	0.796	□	◪

$D/d = 0.28$

(e) flat-type

$Fz_m/\rho_w g H_I D^2$

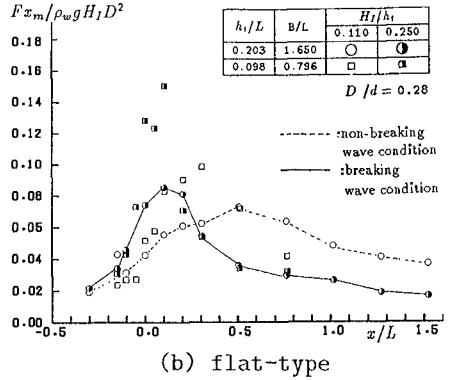| h_t/L	B/L	H_I/h_t	
		0.110	0.250
0.203	1.650	○	◑
0.098	0.796	□	◪

$D/d = 0.28$

(f) edged-type

Figure 3: Variations of $Fx_m/\rho g D^2 H_I$ and $Fz_m/\rho g D^2 H_I$ with x/L.

Fx_{st}/Fx_{sp}

(a) horizontal wave force

● round-type
▲ flat-type
■ edged-type

$D/d = 0.236$
$h_t/L = 0.131$
$H_I/h_t = 0.370$

Fz_{st}/Fz_{sp}

(b) vertical wave force

● round-type
▲ flat-type
■ edged-type

$D/d = 0.236$
$h_t/L = 0.131$
$H_I/h_t = 0.370$
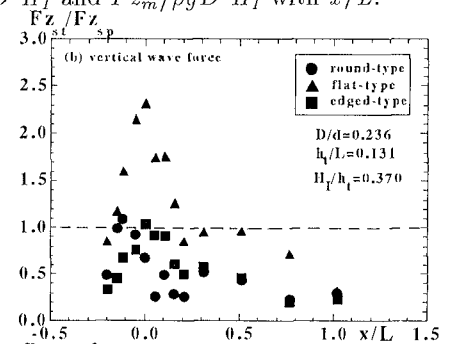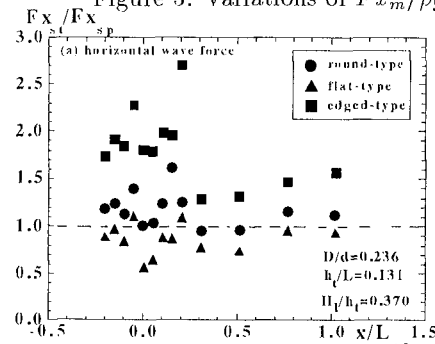
Figure 4: Shape effect of stones.
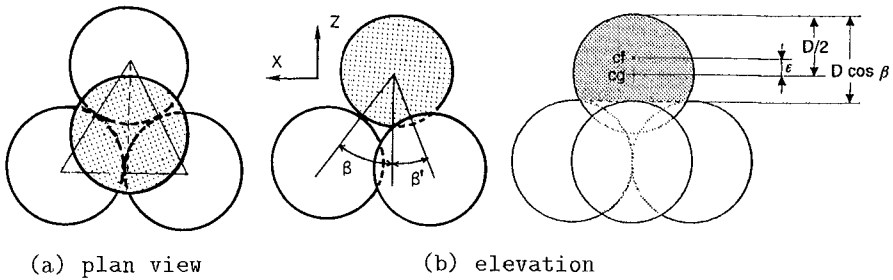
(a) plan view   (b) elevation

Figure 5: Arrangement of spherical units.

the cross-sectional area in the flow direction.

4. STABILITY MODEL OF SPHERICAL ARMOR UNIT

The stability models for spherical armor unit were derived by the present authors (Mizutani et al. 1992); however, the proposed models were applicable only for a given experimental conditions and not suitable for the case of the actual rubble stones. Therefore, in this study, a more general stability model for spherical armor unit for various types of movements were derived in the following manner. By considering an element consisting of four spherical units of the most densely packed arrangement, as shown in Fig. 5, the possible movements of the sphere resting on top of the pyramid formed by the assemblage of these four spheres are rolling, sliding, and uplifting. For sliding and rolling movements, a maximum external force is required to move the sphere along the median line connecting the vertex of the triangle; whereas, a minimum external force is necessary to move the sphere along the median line connecting the base of the triangle. Furthermore, the case of the most movable arrangement of the exposed armor unit also depends on the direction of movement (onshore and offshore). Based on these methodologies, the theoretical models were developed for these two typical cases, CASE-I and CASE-II, as shown in Fig. 6. The uplifting motion was not observed in the experiment proper for the given samples of armor unit, thus, the succeeding models were derived based on rolling and sliding movements only.

By considering the balance of moments for rolling movement and balance of forces for sliding movement, as shown in Fig. 7, the following stability models for spherical armor unit on a submerged breakwater are summarized as follows:

• Stability model for offshore rolling (CASE-I)

$$W_1' \geq \{(\tan\beta)Fn - [1 + (2\varepsilon/D)/\cos\beta]\,Ft\}_m /(\tan\beta - \tan\theta)(\cos\theta) \qquad (1)$$

• Stability model for offshore rolling (CASE-II)

$$W_2' \geq \{(\tan\beta)Fn - 2[1 + (2\varepsilon/D)/\cos\beta]\,Ft\}_m /(\tan\beta - 2\tan\theta)(\cos\theta) \qquad (2)$$
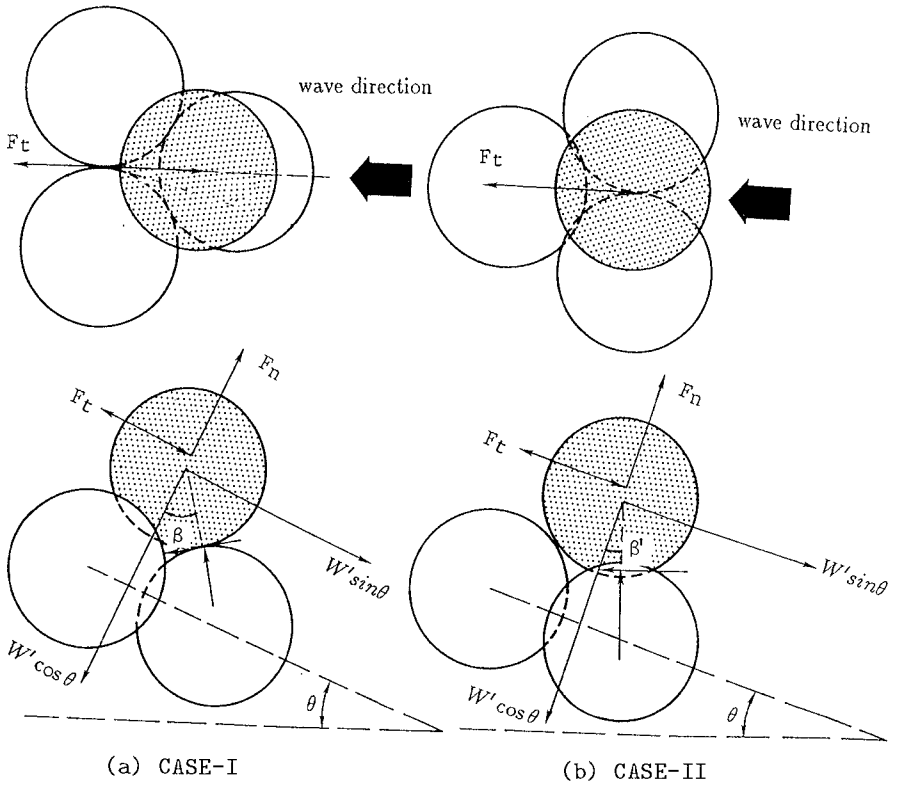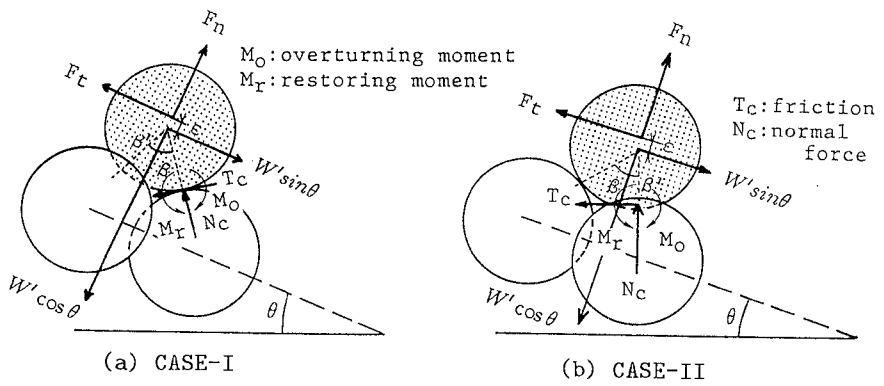
Figure 6: Methods of placement.

Figure 7: Balance of moments and forces.

● Stability model for onshore rolling (CASE-I)

$$W_3' \geq \left\{ (\tan \beta) Fn + 2 \left[1 + (2\varepsilon/D)/\cos \beta \right] Ft \right\}_m / (\tan \beta + 2 \tan \theta)(\cos \theta) \qquad (3)$$

● Stability model for onshore rolling (CASE-II)

$$W_4' \geq \left\{ (\tan \beta) Fn + \left[1 + (2\varepsilon/D)/\cos \beta \right] Ft \right\}_m / (\tan \beta + \tan \theta)(\cos \theta) \qquad (4)$$

● Stability model for offshore sliding (CASE-I)

$$W_5' \geq \frac{\left\{ (\sin \beta + \mu \cos \beta) Fn - (\cos \beta - \mu \sin \beta) Ft \right\}_m}{(\cos \theta \sin \beta - \sin \theta \cos \beta) + \mu(\cos \theta \cos \beta + \sin \theta \sin \beta)} \qquad (5)$$

● Stability model for offshore sliding (CASE-II)

$$W_6' \geq \frac{\left\{ (\sin \beta + 2\mu \cos \beta') Fn - (\cos \beta - \mu \sin \beta') 2Ft \right\}_m}{(\cos \theta \sin \beta - 2\sin \theta \cos \beta) + 2\mu(\cos \theta \cos \beta' + \sin \theta \sin \beta')} \qquad (6)$$

● Stability model for onshore sliding (CASE-I)

$$W_7' \leq \frac{\left\{ (\sin \beta + 2\mu \cos \beta') Fn + 2(\cos \beta - \mu \sin \beta') Ft \right\}_m}{(\cos \theta \sin \beta + 2\sin \theta \cos \beta) + 2\mu(\cos \theta \cos \beta' - \sin \theta \sin \beta')} \qquad (7)$$

● Stability model for onshore sliding (CASE-II)

$$W_8' \leq \frac{\left\{ (\sin \beta + \mu \cos \beta) Fn + (\cos \beta - \mu \sin \beta) Ft \right\}_m}{(\cos \theta \sin \beta + \sin \theta \cos \beta) + \mu(\cos \theta \cos \beta - \sin \theta \sin \beta)} \qquad (8)$$

where subscript $_m$ indicates the maximum value, Fn and Ft are the normal and tangential wave forces, respectively, β and β' are the contact angles defined in Fig. 6, μ is the coefficient of friction, θ is the slope angle of the submerged breakwater ($\theta = 0°$ on the crown), and ε is the eccentricity and location of the center of action of wave force. In this study, the treatment of offshore rolling and offshore sliding for both CASE-I and CASE-II is the same with the work of Lee et al. (1990).

Figure 8 shows the concept of the stability conditions. The domain bounded by the critical stability lines is the stable range; thus, in the case that the trace of wave force is inside the domain, the armor unit is said to be stable. However, as the trace of wave force touches the critical stability lines, the corresponding incipient movement occurs. And beyond the critical stability lines, unstable state of the armor unit is attained.

The comparison between the calculated and experimental values of stable weight for CASE-I on the crown is shown in Fig. 9(a). By following the video-movement analysis, all movements were observed to be onshoreward rolling; thus, the corresponding critical weight given by Eq. 3 is used for the computed values. The calculated value, neglecting the eccentricity and friction, is obtained by substituting the time-varying wave forces into Eq. 3 and taking the maximum value, then, the maximum value for each run was plotted. Some scattering for each period was observed in the maximum wave force, and this
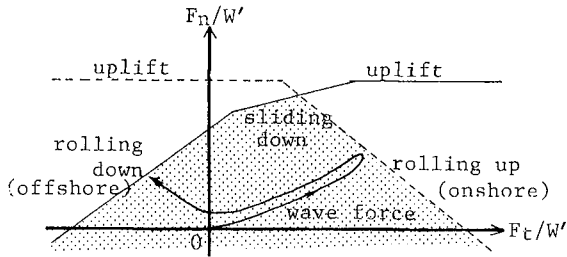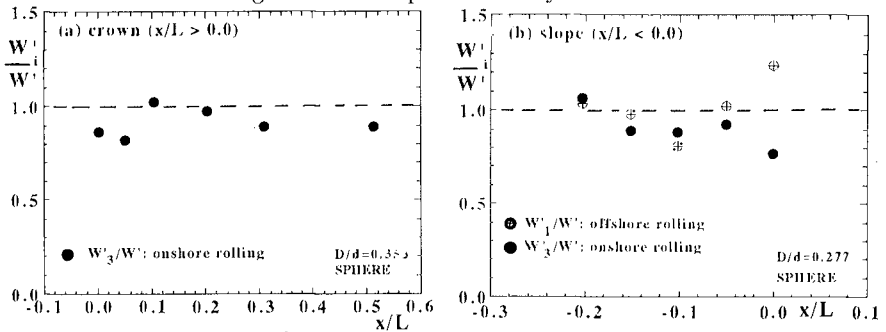
Figure 8: Concept of stability conditions.

Figure 9: Estimated and experimental values for spherical armor unit.

scattering is significant in the movement of the armor unit. On the slope, as shown in Fig. 9(b), both onshore and offshore rolling movements were observed; thus, the calculated values are based on these two movements. These two directions of rolling movements occurred because on the slope, downward movement is likely to prevail; however, the onshore wave force is generally greater than the offshore wave force, as described in Fig. 3, thus, onshore movement is also evident. Although there are some discrepancies between the calculated and experimental values because of the non-uniformity of the slope of the structure, the calculated values generally agree well with the experimental value. Thus, the models derived in this study express well the stable weight of the spherical armor unit.

5. STABILITY MODEL OF ARMOR RUBBLE STONE

A straightforward application of the stability formulae of the spherical armor unit to the armor rubble stone is quite difficult because the shape effect and contact angle vary for a given stone. Thus, some modifications with theoretical consideration and engineering point of view are considered. In this study, only the physical quantities which has a major influence on the movement of the armor stone were included.

For rolling-type movement, the important quantities considered were the acting wave force and the moment-arm lengths. Representing the arm lengths

of the overturning and restoring moments by the maximum tangential and normal lengths, the following models were summarized and given as:
• Stability model for offshore rolling (CASE-I)

$$W_1' \geq \frac{\{Fn - L_eS(1 + \varepsilon/L_2K)Ft\}_m}{(\cos\theta - L_eS\sin\theta)} \tag{9}$$

• Stability model for offshore rolling (CASE-II)

$$W_2' \geq \frac{\{Fn - 2L_eS(1 + \varepsilon/L_2K)Ft\}_m}{(\cos\theta - 2L_eS\sin\theta)} \tag{10}$$

• Stability model for onshore rolling (CASE-I)

$$W_3' \geq \frac{\{Fn + 2L_eS(1 + \varepsilon/L_2K)Ft\}_m}{(\cos\theta + 2L_eS\sin\theta)} \tag{11}$$

• Stability model for onshore rolling (CASE-II)

$$W_4' \geq \frac{\{Fn + L_eS(1 + \varepsilon/L_2K)Ft\}_m}{(\cos\theta + L_eS\sin\theta)} \tag{12}$$

For sliding-type movement, the acting wave force, friction and contact angles were considered important. However, the accurate estimation of the contact angle is complicated for the case of the actual stone. Thus, in the computation, the contact angle can be assumed equal to zero for conservative estimation. The following sliding models are summarized and given as:
• Stability model for offshore sliding (CASE-I)

$$W_5' \geq \frac{\{Fn(\sin\beta + \mu\cos\beta) - Ft(\cos\beta - \mu\sin\beta)\}_m}{(\cos\theta\sin\beta - \sin\theta\cos\beta) + \mu(\cos\theta\cos\beta + \sin\theta\sin\beta)} \tag{13}$$

• Stability model for offshore sliding (CASE-II)

$$W_6' \geq \frac{\{Fn(\sin\beta + 2\mu\cos\beta') - 2Ft(\cos\beta - \mu\sin\beta')\}_m}{(\cos\theta\sin\beta - 2\sin\theta\cos\beta) + 2\mu(\cos\theta\cos\beta' + \sin\theta\sin\beta')} \tag{14}$$

• Stability model for onshore sliding (CASE-I)

$$W_7' \geq \frac{\{Fn(\sin\beta + 2\mu\cos\beta') + 2Ft(\cos\beta - \mu\sin\beta')\}_m}{(\cos\theta\sin\beta + 2\sin\theta\cos\beta) + 2\mu(\cos\theta\cos\beta' - \sin\theta\sin\beta')} \tag{15}$$

• Stability model for onshore sliding (CASE-II)

$$W_8' \geq \frac{\{Fn(\sin\beta + \mu\cos\beta) + Ft(\cos\beta - \mu\sin\beta)\}_m}{(\cos\theta\sin\beta + \sin\theta\cos\beta) + \mu(\cos\theta\cos\beta - \sin\theta\sin\beta)} \tag{16}$$

where $L_e = L_2/L_1$, $S = \cot\beta$, $K = \cos\beta/2$, and the relation between the contact angles, β and β', is given by $\tan\beta = 2\tan\beta'$; for sphere, $L_e = 1.0$. In the above mentioned formulae, W' is the weight of stone in water, and for the weight of armor rubble stone in air, W, the following equation is given.

$$W = W' + \rho V = W'(1 + \frac{\rho}{\rho_s}) \tag{17}$$

where V is the volume of stone and ρ_s is the density of stone.

6. APPLICATION OF STABILITY MODEL

The movements observed for armor stone were rolling and sliding with no uplifting movements. The type of movement depends largely on shapes of stones and location on the structure. On the crown, onshoreward rolling was generally observed for round-type and edged-type of stones. For the case of flat-type stones, onshoreward sliding was generally observed for $D/d = 0.236$ and 0.353; whereas, for $D/d = 0.277$ onshore rolling was always observed. Regardless of shape and size of stone, offshoreward movement was not observed on the crown. On the slope, only rolling motion was generally observed for round-type and edged-type of stones, the direction of movement was almost onshoreward because the onshore wave force is predominant over the offshore wave force. However, there are some cases that offshoreward movement was observed, since armor unit is easily moved in offshoreward direction (down the slope) due to gravitational effect.

The validity of the derived models was examined by comparing the weight of each sample with the estimated weight. Although there is no clear classification of CASE-I and CASE-II for the actual stones, comparison between these two arrangements is made for analysis.

For round-type stones on the crown, the model given by Eq. (11), as shown in Fig. 10(a), for onshoreward rolling for CASE-I generally gives a good estimate although small scattering of data was observed. Figure 10(a) also shows the comparison for the case of the edged-type of stones; the model based on CASE-I arrangement overestimates the actual value. This is attributed to the effect of interlocking between stones, thus, movement is relatively difficult for the same acting wave force. However, the model based on CASE-II arrangement can estimate well the stable weight of the edged-type stone. Therefore, the stable weight of the round-type and edged-type stones can be estimated by Eq. (11) and (12), respectively. The present results suggest that the shape effect is clearly recognized by referring to the arrangement of the spherical armor unit which is the basis of the models derived for rubble stones. Figure 10(b) gives the comparison of stable weight for onshoreward sliding, in this study, $\mu = 0.60$ is used. The model based on the contact angle of sphere, $\beta = 35.26°$, underestimates the actual values; whereas, the model with $\beta = 0.0°$ gives good agreement. Therefore, the model based on CASE-I for onshore sliding with $\beta = 0.0°$ can estimate well the stable weight of flat-type stone.

The onshore movements on the slope were also analyzed. Figure 11(a) shows the comparison between the actual value and the estimated weight based on CASE-I for round-type and edged-type of stones. Although the number of data is limited, the model estimate well the stable weight. The estimated weight based on CASE-II overestimates the stable weight. On the slope, the
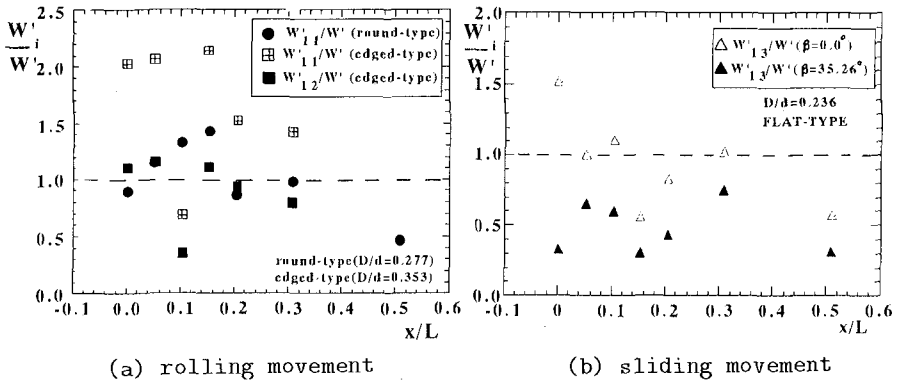
(a) rolling movement   (b) sliding movement

Figure 10: Estimated and experimental values for armor stones on the crown.

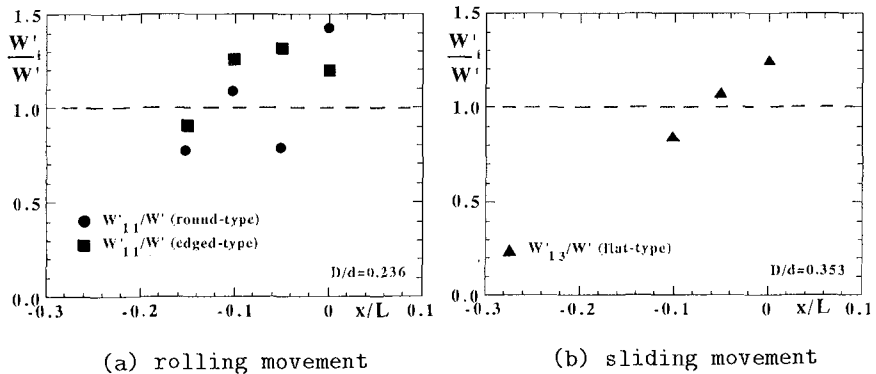(a) rolling movement   (b) sliding movement

Figure 11: Estimated and experimental values for armor stones on the slope.

shape effect of the edged-type stone was not so clear as in the case on the crown. This can be attributed to the contribution of the vertical wave force because on the slope the acting vertical wave force is almost upward when the onshoreward wave force takes its maximum value at incipient motion; consequently, the weight of stone is reduced, thereby, reducing the resistance against rolling. For flat-type stone, the model for offshoreward sliding based on CASE-I gives a good estimate of the stable weight, as shown in Fig. 11(b).

Summarizing these results, the recommended models for each shape of stone are given in Table 3.

7. SIMPLIFICATION OF STABILITY MODEL

The proposed models express the stable weight as a function of both the tangential and normal wave force components. Thus, it is convenient to express the stable weight as a function of only one wave force component. The orthogonal wave forces are correlated by a linear relationship as given in the following equation.

Table 3 Summary of recommended stability models.

STONE SHAPES	LOCATION	MOVEMENT	DIRECTION	STABILITY FORMULA	REMARKS
ROUND TYPE	SLOPE	ROLLING	ONSHORE	Equation 11	
			OFFSHORE	Equation 9	
	CROWN	ROLLING	ONSHORE	Equation 11	
FLAT TYPE	SLOPE	SLIDING	OFFSHORE	Equation 13	$\beta = 0.0°$
	CROWN	ROLLING	ONSHORE	Equation 11	
		SLIDING	ONSHORE	Equation 15	$\beta = 0.0°$
EDGED TYPE	SLOPE	ROLLING	ONSHORE	Equation 11	
			OFFSHORE	Equation 9	
	CROWN	ROLLING	ONSHORE	Equation 12	

$$Fn_m = \phi Ft_m \tag{18}$$

where ϕ is the coefficient. This assumption is based on the experimental results that the movement occurs at the phase that the tangential wave force takes almost a maximum value. Then, if the normal wave force at the phase is expressed in terms of the tangential wave force, the normal wave force can be eliminated. Based on the result, the coefficient ϕ is taken equal to unity for engineering point of view. This means that the normal wave force is almost the same magnitude with the tangential wave force, a phenomenon which corresponds to the most dangerous condition for armor stability. This result was confirmed in some cases but in other cases, the vertical wave force is overestimated. However, the variations of the maximum wave force for each wave period exist even in the case of the regular wave train, and this effect has a significant contribution in the stability of armor unit. On the other hand, it is very difficult to estimate such variation of maximum wave force and mean value of the maximum wave force may be available as an input data. Consequently, the assumption, $Fn_m \simeq Ft_m$, does not overestimate the stable weight, as shown in Fig. 12, where $W'(t)_m$ is the computed stable weight using the maximum time varying quantity of the right-hand side of the corresponding model, and $W'(Ft)_m$ is the computed stable weight using the relation that the maximum normal is approximately equal to maximum tangential wave force.

Substituting the variation of maximum wave forces into the respective models, depending on the arrangement, the distribution of the stable weight of typical shape of stone along the submerged breakwater is obtained, as given in Fig. 13. It is noted that there is no significant differences among the three shapes of stones, although the shape effect was evident in wave force and stability. This implies that the shape effect of armor unit has a significant influence on wave force and moving limitations, but, for the case of stable weight, the shape effect due to the wave force and moving limitations cancel each other.
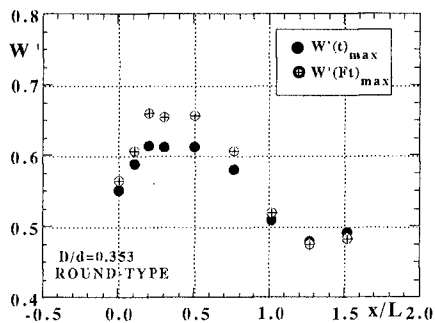
Figure 12: Validity of the assumption, $Fn_m \simeq Ft_m$.

(a) round-type ($D/d = 0.353$)

(b) round-type ($D/d = 0.236$)

(c) flat-type ($D/d = 0.353$)

(d) flat-type ($D/d = 0.236$)

(e) edged-type ($D/d = 0.353$)

(f) edged-type ($D/d = 0.236$)
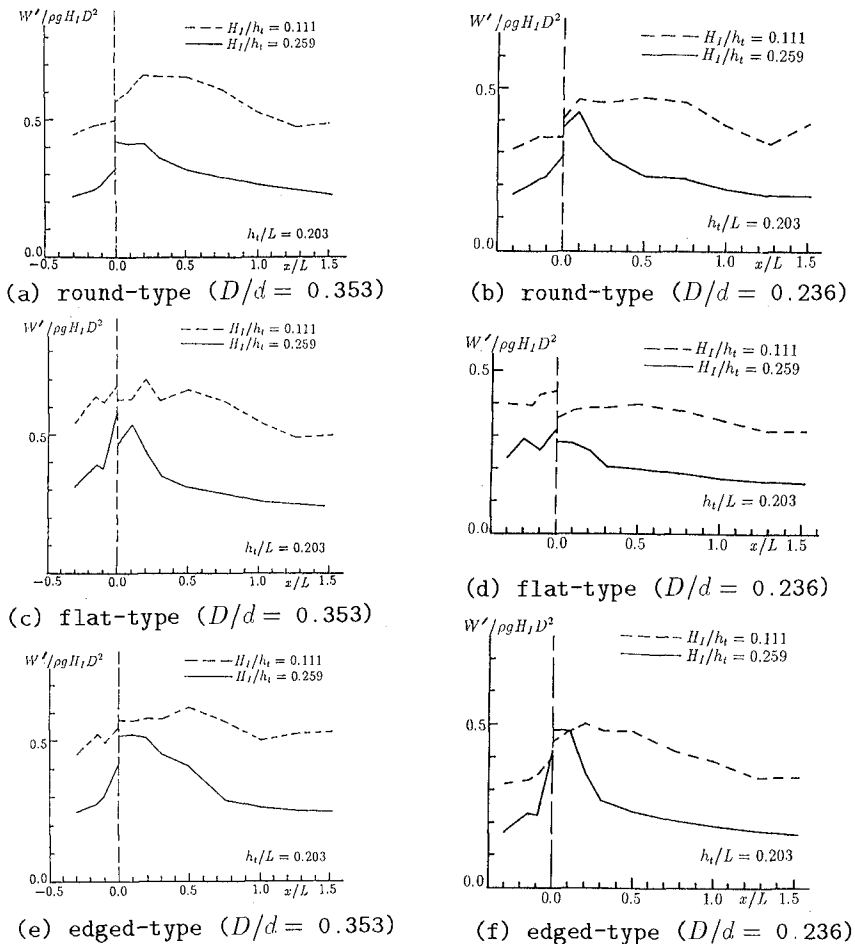
Figure 13: Stability distribution of armor stones.

8. CONCLUSIONS

Significant results are summarized as follows:

(1) A general stability models were derived based on acting wave forces, moment-arm lengths and contact angles.

(2) The vicinity around the crown-edge is revealed to be the most critical location on the submerged breakwater.

(3) Large cross-sectional area enlarges the wave force.

(4) To consider the moment-arm length and contact angle, the stability model for spherical armor unit can be applicable to the armor stone.

(5) The stable weight is not so affected by the stone shape since the shape effect on the stability is offset by the shape effect of the acting wave force.

ACKNOWLEDGMENT

REFERENCES

[1] Brebner, A. and Donnelly, P. (1962). "Laboratory study of rubble foundations for vertical breakwaters," *Proc., 8th Coastal Engrg. Conf., ASCE*, pp. 408-429.

[2] Hedar, P. A. (1986). "Armor layer stability of rubble-mound breakwaters," *J. of Waterway, Port, Coastal, and Ocean Engrg., ASCE*, Vol. 112, No. 3, pp. 343-350.

[3] Hudson, R. Y. (1958). "Design of quarry-stone cover layers for rubble-mound breakwaters," *Technical report, Waterways Experiment Station Research*, No. 2-2.

[4] Hudson, R. Y. (1959). "Laboratory investigation of rubble-mound breakwaters," *J. of Waterway, Port, Coastal, and Ocean Engrg., ASCE*, Vol. 85, pp. 93-121.

[5] Iwata, K., Miyazaki, Y. and Mizutani, N. (1985). "Experimental study of the wave force acting on armour rubble of a rubble-mound slope," *Proc., Natural Disaster Science*, Vol. 7, No. 2, pp. 29-41.

[6] Lee, S. W., McDougal, W. G., Sulisz, W., and Sollitt, C. K. (1990). "Stability of Rubble Toe," *Engineering Report, Department of Civil Engrg., OSU*, 117 pp.

[7] Mizutani, N., Iwata, K., Rufin, T.M. Jr., and Kurata, K. (1992). "Laboratory investigation on the stability of a spherical armor unit of submerged breakwater," *Proc., 23rd Coastal Engrg. Conference, ASCE*, pp. 1400-1413.

[8] Rufin, T.M. Jr., Mizutani, N., and Iwata, K. (1993). "Stability model of a spherical armor unit of a submerged breakwater," *Proc., 25th International Association for Hydraulic Research*, Vol. 4, pp. 190-197.

[9] Rufin, T.M. Jr., Mizutani, N., Totsuka, N., Kurata, K., and Iwata, K. (1994)." Wave forces acting on armor unit of a submerged wide-crown breakwater," *Proc., 4th International Offshore and Polar Engrg., ISOPE*, Vol. 3, pp. 556-563.

[10] Tørum, A. (1994). "Wave-induced forces on armor unit on berm breakwaters," *J. of Waterway, Port, Coastal, and Ocean Engrg., ASCE*, Vol. 120, pp. 251-268.

[11] Uda, T., Omata, T., and Saito, T. (1989). "Design formula for weight of armor unit for an artificial reef," *Proc., Japanese Conference on Coastal Engrg., JSCE*, Vol.36, pp. 648-652 (in Japanese).